Water Research 106 (2016) 1–14

Contents lists available at ScienceDirect

Water Research

journal homepage: www.elsevier.com/locate/watres

Effectiveness of hypolimnetic oxygenation for preventing accumulation of Fe and Mn in a drinking water reservoir

Zackary W. Munger [a, *], Cayelan C. Carey [b], Alexandra B. Gerling [b], Kathleen D. Hamre [b], Jonathan P. Doubek [b], Spencer D. Klepatzki [a], Ryan P. McClure [b], Madeline E. Schreiber [a]

[a] Department of Geosciences, Virginia Tech, Derring Hall, 24061, Blacksburg, VA, USA
[b] Department of Biological Sciences, Virginia Tech, Derring Hall, 24061, Blacksburg, VA, USA

ARTICLE INFO

Article history:
Received 2 July 2016
Received in revised form
16 August 2016
Accepted 20 September 2016
Available online 20 September 2016

Keywords:
Iron
Manganese
Anoxia
Reservoir
Oxygenation
Water quality management

ABSTRACT

The accumulation of Fe and Mn in seasonally stratified drinking water reservoirs adversely impacts water quality. To control issues with Fe and Mn at the source, some drinking water utilities have deployed hypolimnetic oxygenation systems to create well-oxygenated conditions in the water column that are favorable for the oxidation, and thus removal, of Fe and Mn. However, in addition to being controlled by dissolved oxygen (DO), Fe and Mn concentrations are also influenced by pH and metal-oxidizing microorganisms. We studied the response of Fe and Mn concentrations to hypolimnetic oxygenation in a shallow drinking water reservoir in Vinton, Virginia, USA by sequentially activating and deactivating an oxygenation system over two summers. We found that maintaining well-oxygenated conditions effectively prevented the accumulation of soluble Fe in the hypolimnion. However, while the rate of Mn oxidation increased under well-oxygenated conditions, soluble Mn still accumulated in the slightly acidic to neutral (pH 5.6 to 7.5) hypolimnion. In parallel, we conducted laboratory incubation experiments, which showed that the presence of Mn-oxidizing microorganisms increased the rate of Mn oxidation in comparison with rates under oxic, abiotic conditions. Combined, our field and laboratory results demonstrate that increasing DO concentrations in the water column is important for stimulating the oxidation of Fe and Mn, but that the successful management of Mn is also tied to the activity of Mn-oxidizing organisms in the water column and favorable (neutral to alkaline) pH.

1. Introduction

Controlling iron (Fe) and manganese (Mn) in drinking water is a complex challenge for water utilities because of the adverse effects of these metals on drinking water quality and the difficulties in preventing their accumulation in source reservoirs. Issues with water staining, odor, and taste can be attributed to elevated Fe and Mn concentrations (Sommerfeld, 1999; World Health Organization, 2004), and adverse human health effects have also been associated with chronic exposure from drinking water (Wasserman et al., 2006). In response to the aesthetic water quality effects, the World Health Organization (WHO) has established guidelines for Fe and Mn concentrations in drinking water at 0.3 and 0.1 mg/L, respectively (World Health Organization, 2004). In the United States, the United States Environmental Protection Agency (EPA) has established secondary maximum contaminant limits for Fe and Mn concentrations in drinking water at 0.3 and 0.05 mg/L, respectively (United States Environmental Protection Agency, 2016). Treatment of Fe and Mn is most commonly accomplished by oxidation and filtration techniques (Kohl and Medlar, 2006; Sommerfeld, 1999); however, the accumulation of these metals in raw water increases the cost and difficulty of the water treatment process.

The development of reducing conditions in lake and reservoir sediments during thermal stratification leads to the reductive dissolution of Fe and Mn from the sediments and subsequent diffusion of these metals into the water column (Davison, 1993; Hem, 1972). Under oxidizing conditions (dissolved oxygen (DO) concentrations >2 mg/L), Fe and Mn occur naturally as oxidized, insoluble forms (Fe^{3+}, Mn^{3+}, and Mn^{4+}) in watershed sediments (Jones and Bowser, 1978). However, anoxic conditions (DO concentrations < 0.5 mg/L) commonly develop within the sediments of lakes and reservoirs during thermal stratification that are

* Corresponding author. 4044 Derring Hall, Blacksburg, VA 24061, USA.
E-mail address: mzacka@vt.edu (Z.W. Munger).

http://dx.doi.org/10.1016/j.watres.2016.09.038
0043-1354/

favorable for the reduction of Fe and Mn to soluble forms (Fe^{2+} and Mn^{2+}; Davison, 1993; Lerman et al., 1995). The reduction of Fe and Mn is known to occur abiotically via redox reactions with sulfides, organic acids, and Fe^{2+} (Mn reduction only); however, microbial activity also plays an important role in metal reduction through the production of sulfide, organic acids, and anaerobic respiration, which couples the mineralization of organic carbon to Fe and Mn reduction (Burdige, 1993; Lovley, 1987; Nealson and Saffarini, 1994). Reductive dissolution of Fe and Mn causes accumulation of soluble Fe and Mn in anoxic sediment pore waters, where concentration gradients drive their diffusion into the overlying water column (Davison, 1993; Hongve, 1997; Zaw and Chiswell, 1999). Transport of reduced Fe and Mn back into oxidizing zones in the sediments or water column can lead to these metals becoming oxidized, often precipitating as insoluble Fe- and Mn-oxyhydroxides that are subject to sedimentation out of the water column (Davison, 1993; Hem, 1972).

Hypolimnetic oxygenation is increasingly used as the first stage in treating Fe and Mn *in situ* by maintaining well-oxygenated conditions in the hypolimnion of seasonally stratified lakes and reservoirs (Beutel and Horne, 1999; Bryant et al., 2011; Burns, 1998; Debroux et al., 2012; Dent et al., 2014; Gantzer et al., 2009; Gerling et al., 2014). Hypolimnetic oxygenation (HOx) systems increase DO concentrations by injecting air, pure oxygen, or oxygenated water into the hypolimnion (Beutel and Horne, 1999; Gerling et al., 2014; Singleton and Little, 2006). Physical mixing induced by the HOx system operation often accompanies the injection of oxygen, aiding in distributing DO throughout hypolimnion (Fig. 1; Beutel and Horne, 1999; Gantzer et al., 2009; Gerling et al., 2014). Successful management Fe and Mn using hypolimnetic oxygenation depends on maintaining a sufficiently oxidizing environment to quickly precipitate oxidized metals in the water column, where they will settle back to the bottom sediments, or ideally, to cause metals to precipitate prior to being released from the sediment pore waters into the hypolimnion water column.

The rate of metal oxidation in the water column is primarily influenced by DO concentrations, pH, and microbial activity (Diem and Stumm, 1984; Hem, 1981, 1972). The abiotic oxidation of Fe is faster than Mn under similar DO and pH conditions. For example, in air-saturated water with pH > 6, abiotic Fe oxidation is rapid, with soluble Fe having a half-time, defined as the time required for half of the initial mass of soluble Fe to become oxidized, of < 24 h (Davison, 1993). However, under similar conditions the half-time for soluble Mn can be > 1 year (Morgan, 1967). Soluble Mn oxidation occurs much faster in oxic lake water than observed under abiotic conditions, with several studies observing soluble Mn oxidation half-times between 1 and 30 days at pH between 6.5 and 8.4 (Chapnick et al., 1982; Diem and Stumm, 1984; Kawashima et al., 1988; Tipping et al., 1984). Chapnick et al. (1982) and Diem and Stumm (1984) identified Mn-oxidizing organisms in the reservoir water and showed that when these organisms were removed by filtration, Mn oxidation was negligible within the duration of their incubation experiments (10–30 days). The mechanisms of biotic Mn oxidation are not fully understood, but there is evidence that strains of actinobacteria, cyanobacteria, firmicutes, proteobacteria, and fungi have some ability to cause Mn oxidation and are ubiquitous in aquatic environments (Aguilar and Nealson, 1998; Richardson et al., 1988; Tebo et al., 2005), suggesting that the rates of Mn oxidation in lakes and reservoirs are strongly influenced by the activity of Mn-oxidizing organisms.

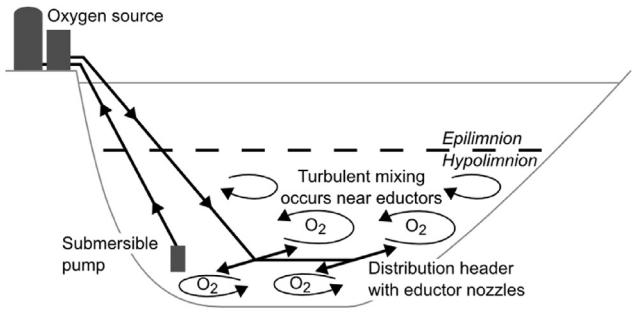

Fig. 1. Hypolimnetic oxygenation systems cause turbulence in the water column that may lead to physical mixing of the hypolimnion. This figure depicts the mixing induced by the side-stream supersaturation system installed in FCR. This figure is adapted from Gerling et al. (2014).

Although decreased concentrations of Fe and Mn have been observed in oxygenated reservoirs, sediments can continue to release metals, even in oxic hypolimnia (Aguilar and Nealson, 1998; Bryant et al., 2011; Gantzer et al., 2009). For example, Gantzer et al. (2009) reported a 97% decrease in Mn concentrations in the hypolimnion of Carvins Cove, Virginia, USA following the installation and continuous operation of a HOx diffuser system. However, elevated Mn concentrations were still observed in the sediment pore waters while the overlying hypolimnion was well-oxygenated, indicating that upward diffusion of Mn mass continued during HOx operation (Bryant et al., 2011; Gantzer et al., 2009). Similarly, Dent et al. (2014) reported decreases of the mean hypolimnetic Fe and Mn concentrations in North Twin Lake, Washington, USA, by 71% and 73%, respectively, within 8 h of activating the oxygenation system; however, the mean concentrations reported in that study did not account for volume difference along the profile, which makes it difficult to determine whether the decrease in hypolimnetic metal concentrations can be attributed to rapidly enhanced oxidation or whether redistribution of mass in response to HOx-induced physical mixing also influenced concentrations along the depth profile.

Managing Fe and Mn treatment in drinking water systems is challenging and expensive. Thus, accurately characterizing the processes controlling metal removal in drinking water reservoirs at the whole-ecosystem scale is needed to optimize management strategies. As discussed above, metal concentrations are affected by a host of biogeochemical and physical processes in waterbodies (Aguilar and Nealson, 1998; Bryant et al., 2011; Diem and Stumm, 1984; Gantzer et al., 2009). While previous studies have examined the impacts of specific processes of metal concentrations in laboratory incubations or examined larger scale patterns at the lake or reservoir scale (Beutel et al., 2008; Diem and Stumm, 1984; Gantzer et al., 2009; Gerling et al., 2014), it remains unknown how redox and pH-dependent processes in the water column and sediments, physical mixing across concentration gradients, and the activity of metal-oxidizing bacteria together affect metal concentrations at the reservoir scale.

The goal of this study was to investigate the effects of hypolimnetic oxygenation on Fe and Mn oxidation at the whole-ecosystem scale in a drinking water reservoir. We manipulated the HOx system to experimentally create intermittent periods of hypolimnetic anoxia and well-oxygenated conditions over two years. Throughout the two-year experiment, we measured the effects of HOx system activation on soluble and total Fe and Mn accumulation in the hypolimnion and the rate of particulate metal sedimentation. In parallel, we conducted laboratory incubation experiments to evaluate the influence of microbial activity on Mn oxidation in the reservoir. We used the field and laboratory data to evaluate the importance of biogeochemical processes in Fe and Mn oxidation in oxygenated reservoirs.

2. Methods

2.1. Study site

Falling Creek Reservoir (FCR) is a shallow (maximum depth = 9.3 m, mean depth = 4 m, surface area = 0.119 km^2, volume of 3.1 × 10^5 m at full pond), eutrophic drinking water reservoir owned and managed by the Western Virginia Water Authority (WVWA) and located in a forested watershed in southwestern Virginia, USA, as shown in Fig. 2. The primary source of water to the reservoir is a surface water stream that enters along the northeastern shoreline (Gerling et al., 2016). FCR is moderately eutrophic and typically experiences thermal stratification between April and October, during which time the hypolimnion develops anoxic conditions (Gerling et al., 2016, 2014).

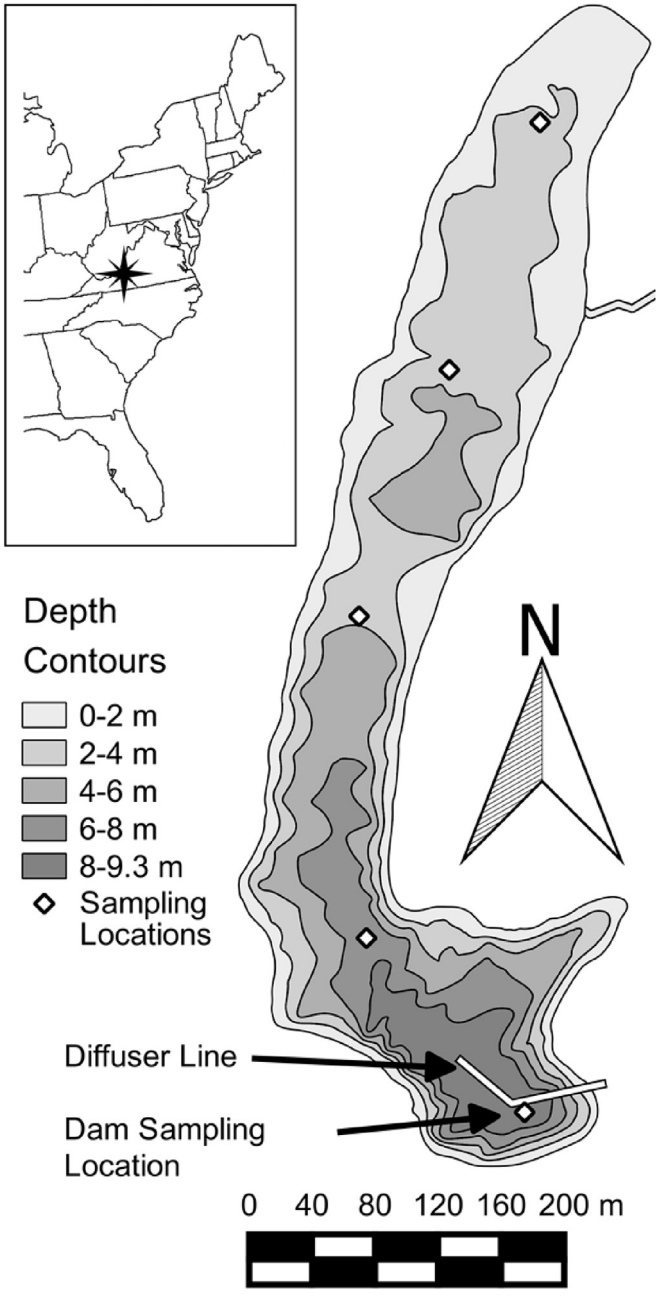

Fig. 2. Falling Creek Reservoir bathymetry, location of oxygenation system diffuser lines, and water sample collection sites.

2.2. Hypolimnetic oxygenation system description

In autumn 2012, a side-stream supersaturation hypolimnetic oxygenation system was deployed in FCR (see Gerling et al., 2014, for a full system description and analysis of reservoir oxygen demand). The HOx system at FCR consists of a submersible pump (positioned at 8.5 m depth), inlet piping, an oxygen source, an oxygen contact chamber, outlet piping, and distribution headers (positioned at 8.5 m depth). Water is withdrawn from the reservoir via the submersible pump and transferred to the oxygen contact chamber, where it is supersaturated with oxygen supplied by the oxygen source. The water is then transported to the distribution headers via the outlet piping, where it is injected back into the hypolimnion. A schematic showing the side-stream supersaturation HOx system in FCR is depicted in Fig. 1.

The distribution header used 15 evenly-spaced eductor nozzles to promote rapid dilution of the oxygenated water and physical mixing throughout the hypolimnion. For every 1 L of oxygenated water injected through the nozzle, 4 L of hypolimnion water was suctioned through the nozzle. For example, at a flow rate of 10 L/min at the submersible pump, 40 L/min of hypolimnetic water was also being suctioned through the nozzle, giving a total flow through the nozzle of 50 L/min. The distribution header was 76.2 m long, designed to cover the length of the deepest region of the reservoir. The nozzles were angled upwards by 10° from horizontal to minimize sediment disturbance. Additional details about the HOx system in FCR are described in Gerling et al. (2014).

2.3. Oxygenation system operation

To examine the effects of hypolimnetic oxygenation on Fe and Mn concentrations in FCR, we created alternating periods of well-oxygenated and hypoxic (DO < 2 mg/L) conditions in the hypolimnion during the summer stratified period (see Table 1). In both 2014 and 2015, we began operation of the HOx system in early May; the initial period of HOx system activation lasted ~4 weeks. In 2014, the HOx system was deactivated for two extended intervals, following the initial activation period, to allow anoxic conditions to develop at the bottom sediments. After anoxic conditions were established, the HOx system was reactivated to restore oxic conditions in the bottom of the hypolimnion. In 2015, the HOx system was deactivated for one week beginning June 1 and for 1.5 h on July 28; however, the HOx system was continuously operated over the majority of the stratified period to maintain well-oxygenated conditions at the bottom sediments. The oxygen addition rates over both years varied between 12.5 and 25 kg/d (Table 1). The pump flow rate for all oxygenation periods was set at 227 L/min, with a total flow through the eductor nozzles of 1135 L/min. At this flow

Table 1
Dates of activation and oxygen addition rates for the HOx system.

Year	Dates of activation	Oxygen addition rate (kg/d)
2014	May 5–Jun 3	20
2014	Jun 29–Jul 22	20
2014	Aug 18–Nov 10	25
2015	May 5–Jun 1	15
2015	Jun 8–Jun 23	12.5
2015	Jun 23–Jul 27	20
2015	Jul 28–Aug 8	15
2015	Aug 8–Nov 20	20

rate, the hypolimnion volume was circulated through the eductor nozzles every 20–30 days.

2.4. Sample collection and analyses

2.4.1. Metal concentrations, temperature, dissolved oxygen, and pH in reservoir water

We collected water samples to measure total and soluble Fe and Mn along a depth profile at the deepest site in FCR in 2014 and 2015 (see Sampling Location in Fig. 2). Water samples were collected at nine depths in 2014 (0.1, 0.8, 1.6, 2.8, 3.8, 5.0, 6.2, 8.0 and 9.0 m) and seven depths in 2015 (0.1, 1.6, 3.8, 5.0, 6.2, 8.0 and 9.0 m) using a 4 L Van Dorn sampler (Wildlife Supply Company). During our study, water was only withdrawn from the epilimnion for water treatment. Reservoir water samples were collected from the deepest site of the reservoir, adjacent to the dam, shown in Fig. 2. Samples were collected weekly between April and October, and monthly through November in both years. After collection, we poured raw water samples directly into HDPE bottles for total metal analyses and syringe-filtered water using 0.45 μm nylon filters into HDPE bottles for soluble metal analyses. The samples were acidified with trace metal grade nitric acid to pH < 2 to preserve them until analysis. After collection, the samples were analyzed for Fe and Mn using an ICP-MS (Thermo Electron X-Series) following APHA Standard Method 3125-B (American Public Health Association et al., 1998).

We measured temperature and DO concentrations along a depth profile in the water column of FCR in both years at the same site where we collected water samples, as well as upstream at six additional sites on a transect between the reservoir's inflow and dam in FCR (shown on Fig. 2). Temperature and DO were measured using a Seabird Electronics SBE 19plus high-resolution profiler (CTD), which allowed us to collect data at about 0.1 m vertical increments. These sampling sites were the same as those used by Gerling et al. (2014), who found that DO concentrations measured at the deepest site in the reservoir were representative of conditions throughout the reservoir.

To examine how DO concentrations change vertically within the water column as a result of HOx system-induced mixing, we collected a DO profile at the deepest site which was located immediately adjacent to the oxygenation system, right before activation in June 2014, and seven additional DO profiles at 1, 2, 3, 5, 24, 48, and 72 h after HOx system activation.

Measurements of pH were collected weekly during the summer stratified period in 2014 at 0.1, 1.6, 3.8, and 6.2 m depths and at all seven of the sampling depths in 2015 using a YSI multiparameter meter.

The volume-weighted hypolimnetic (VWH) DO and metal concentrations were calculated using bathymetry data from Gerling et al. (2014) and profiles collected in FCR. We first determined the hypolimnetic masses of DO, Fe and Mn by linearly interpolating the measured concentrations in the hypolimnion at the depths in the bathymetry data (~0.3 m intervals) and multiplying the interpolated concentration data by the volume of water in each layer corresponding to those depths. The total hypolimnion mass was the sum of the masses in each layer below the thermocline. The thermocline depth was determined from the CTD temperature profiles collected on each sampling date and analyzed using Lake Analyzer, a Matlab program (Mathworks; Read et al., 2011), and the hypolimnion volume was calculated as the cumulative volume from the sediments to the mean thermocline depth for each year, following Gerling et al. (2014). We calculated the VWH concentrations by dividing the hypolimnion mass by the total volume in the hypolimnion. The mean thermocline depths were 4.1 ± 0.8 m (1 standard deviation) and 4.6 ± 0.9 m in 2014 and 2015, respectively.

2.4.2. Sedimentation traps at 4 m and 8 m depths in the reservoir

We deployed sedimentation traps (KC Denmark A/S) at 4 m and 8 m depth near the dam in FCR to capture particulate metal sedimentation. Each trap contained two tubes with openings of 7.2 cm in diameter. The sedimentation traps were deployed between May–December in 2014 and April–November in 2015, and particulate samples were retrieved every 14 days during summer and every 28 days in autumn. During sampling, the traps were brought to the surface and the mixture of water and particulates was poured into 1 L bottles. The samples in these bottles were vacuum-filtered through pre-weighed glass microfiber filters (1.5 μm; Whatman 934-AH). The filters containing particulates were dried at 45 °C in a drying oven and the retained mass was calculated by difference from the final and starting mass of the filter.

We determined the particulate metal flux by digesting the raw particulate matter retained on the filters and analyzing the digestion solution for Fe and Mn concentrations. The raw particulates were microwave-digested with trace metal grade nitric acid following EPA Method 3051A (United States Environmental Protection Agency, 1995). We analyzed the resulting digestion solution for Fe and Mn using ICP-MS, as described above. The mass of particulate metal was calculated by multiplying the metal concentration by the known volume of acid added to each sample. We calculated the particulate metal sedimentation flux by dividing the trapped metal mass by the trap opening area and duration of trap deployment. Measurement uncertainty was calculated using the standard deviation between the replicate flux measurements at each depth.

We estimated zero-order Fe and Mn oxidation rates in the hypolimnion of FCR using the sediment trap data. To do this, we assumed that the metal sedimentation rate represented the rate of particulate metal production in the water column (via oxidation). To calculate the hypolimnion oxidation rate, we first subtracted the flux calculated at 4 m (allochthonous particulates) from the 8 m flux. The hypolimnion flux ($M/L^2/T$) was divided by the water column thickness between traps (4 m) to calculate an average zero-order oxidation rate (K; $M/L^3/T$) in the hypolimnion. We used the volume-weighted hypolimnion soluble metal concentration at the beginning of the trap deployment interval as the initial concentration (C_0).

Using the zero-order oxidation rate, we then calculated an oxidation “half-time” for each rate, a characteristic time that reflects how long soluble Fe and Mn persist in the hypolimnion of FCR prior to being oxidized and removed via particulate settling. We calculated the oxidation half-time, $t_{i,0.5}$, for both Fe and Mn with the equation (Rimstidt, 2013):

$$t_{0.5} = \frac{0.5C_0}{K} \quad (1)$$

2.5. Manganese oxidation incubations

We designed a laboratory incubation experiment to evaluate the relative influence of biotic and abiotic processes on Mn oxidation in the reservoir. Our experiment had five treatments with four replicates each: 1) a slurry of reservoir particulates spiked with Mn (PMn), 2) reservoir water spiked with Mn (WMn), 3) a slurry of particulates without the Mn spike (P), 4) a slurry of sterilized particulates spiked with Mn (SPMn), and 5) sterilized reservoir water spiked with Mn (SWMn).

We conducted the incubation experiments in 250 mL sterilized Erlenmeyer flasks. Each flask received 100 mL of live or sterilized reservoir water according to its treatment. The particulates and reservoir water used in the experiments were collected in September 2015 from a sedimentation trap deployed at 4 m depth in the same manner as described in Section 2.4.2. The reservoir water (19 °C at collection) was siphoned from the 1 L bottle and 1 mL of the resulting slurry was transferred to the experiment flasks assigned to the particulate treatments. We sterilized the flasks and sample material by autoclaving them at 121 °C for 45 min; the sterilized particulates also received 1 g sodium azide to kill all microorganisms. We spiked the samples with Mn^{2+} using 1 mL aliquot of 250 mg/L $MnCl_2$ aqueous solution. All flasks were covered in aluminum foil and placed on a shaker table in the dark at room temperature (21 °C).

The experiment was sampled at regular intervals to quantify the rate of soluble Mn (Mn^{2+}) loss for 18 days. Three of the flask replicates were sampled for soluble Mn and the fourth replicate was used to measure temperature, pH, and DO concentrations. During sampling, a 1 mL aliquot was collected from each of the three sample replicate flasks at 0.5 h, 3 h, 6 h, 12 h, 1 d, 2 d, and every 3 d between 3 and 18 d using a sterile syringe. Temperature, pH, and DO concentrations were measured in the fourth replicate flasks simultaneous with the water sample collection. After collection, samples were filtered (0.2 μm nylon filter), diluted to 10 mL with deionized water, and preserved with trace metal grade nitric acid. The samples were analyzed for soluble Mn using ICP-AES following EPA Method 200.7 (Creed et al., 1994). Measurement uncertainty was determined using the standard deviation of the triplicate measurement results. We calculated zero-order Mn oxidation rates (K; $M/L^3/T$) by fitting a linear model to the Mn data as described in Rimstidt (2013), assuming that any decrease in soluble Mn concentration was the result of oxidation. The half-time of soluble Mn in the incubations was calculated using the zero-order oxidation rates with Equation (1).

3. Results

3.1. Temperature, dissolved oxygen, and pH in the reservoir

Activation and deactivation of the HOx system successfully established intermittent periods of oxic and anoxic hypolimnetic conditions in 2014 (Fig. 3). In early April 2014, DO concentrations and temperature were relatively uniform throughout the water column. By mid-April, thermal stratification had intensified, causing the volume-weighted hypolimnetic (VWH) DO concentration to decrease at a rate of 0.14 mg/L/d between April and early May. The HOx system was activated in early May 2014 (see Table 1 for HOx system activation dates), which caused the VWH DO concentration to increase at a rate of 0.04 mg/L/d. Over the summer stratified period when the HOx system was deactivated, the VWH DO concentration decreased at a mean rate of 0.16 ± 0.02 mg/L/d (1 SD), which resulted in anoxic conditions (DO < 0.5 mg/L) in the bottom layer of the hypolimnion in June and August. When the system was activated in June/July and August/September, the VWH DO concentration increased at a mean rate of 0.04 ± 0.03 mg/L/d.

Along the depth profile, DO concentrations changed most rapidly in the bottom layer of the hypolimnion in response to HOx system activation (Fig. 3). During the three-day periods after the HOx system was activated in May, June, and August 2014, DO concentrations at 9 m depth increased by a mean rate of 0.67 ± 0.12 mg/L/d, ~30 times faster than the bulk hypolimnion. CTD profiles showed that DO concentrations quickly increased below ~7 m depth and decreased slightly at shallower depths in the hypolimnion after the HOx system was activated (Fig. 5). Within 24 h after HOx system activation, DO concentrations throughout the hypolimnion were uniform due to the system's mixing of anoxic bottom layers with oxic water from shallower depths in the hypolimnion.

Continuous operation of the HOx system maintained oxic conditions for most of the summer stratified period in 2015 (Fig. 3). Similar to 2014, the VWH DO concentration decreased at a rate of 0.13 mg/L/d prior to HOx system activation. After the HOx system was activated in early May, the VWH DO concentration increased at a rate of 0.07 mg/L/d. In 2015, we only observed anoxia in the bottom of the hypolimnion after a one-week period when the HOx system was deactivated in early June. After the HOx system was reactivated in June, the VWH DO concentration remained > 4 mg/L for the rest of the summer stratified period, including a brief, 1.5 h interval when the HOx system was deactivated in July 2015. Despite DO concentrations > 8 mg/L throughout most of the hypolimnion during the summer in 2015, the VWH DO concentration never exceeded ~7 mg/L due to the persistence of anoxia just below the thermocline. In both 2014 and 2015, anoxia developed in the metalimnion and persisted until the water column destratified in autumn, suggesting that physical mixing across the thermocline did not increase substantially when the HOx system was activated.

We found that the DO and temperature conditions measured at the dam sampling site were representative of upstream conditions throughout the reservoir (Fig. 4). As observed by Gerling et al. (2014), activation of the HOx system increased oxygen concentrations throughout the entire hypolimnion, without altering thermal stratification or water temperature. Thus, although we sampled for Fe and Mn along one depth profile near the dam, our DO and temperature data along the reservoir transect support the use of this profile as representative of hypolimnion conditions throughout the reservoir.

During the summer stratified period in 2014 and 2015, we measured a mean pH of 6.8 ± 0.4 (6.2 m depth only in 2014) and 6.2 ± 0.3, respectively, in the hypolimnion (Appendix A). Between April and May in 2014, the pH was ~0.5 units higher than that measured between June and September. Similarly, in 2015 the pH was ~0.2 units higher between April and May compared to pH measured between June and September.

3.2. Iron concentrations in the reservoir water column and sedimentation traps

Total Fe concentrations increased in the hypolimnion during the summer stratified period, even when the HOx system was activated (Fig. 6). During the early stratified period (between April and May) in both 2014 and 2015, total Fe concentrations in the hypolimnion remained ~0.5 mg/L. However, later in the stratified period, between June and September, total Fe concentrations increased throughout the hypolimnion. The average rates at which total Fe concentrations increased between June and September in 2014 (0.016 mg/L/d) and 2015 (0.015 mg/L/d) were similar, despite the higher DO concentrations that were measured during these months on average in 2015 compared to 2014 (Fig. 7). Although the rates of total Fe accumulation in the hypolimnion were similar during intervals of anoxia and well-oxygenated conditions, we measured the highest total Fe concentrations near the bottom of the reservoir (33 mg/L at 9 m depth in August 2014) when the hypolimnion was anoxic in response to HOx system deactivation (Fig. 7). When the HOx system was activated, total Fe concentrations near the bottom of the reservoir were much lower than observed during anoxic intervals; however, the VWH total Fe concentrations reached similar levels regardless of HOx system operation (Fig. 7).

Soluble Fe concentrations were generally low (<1 mg/L)

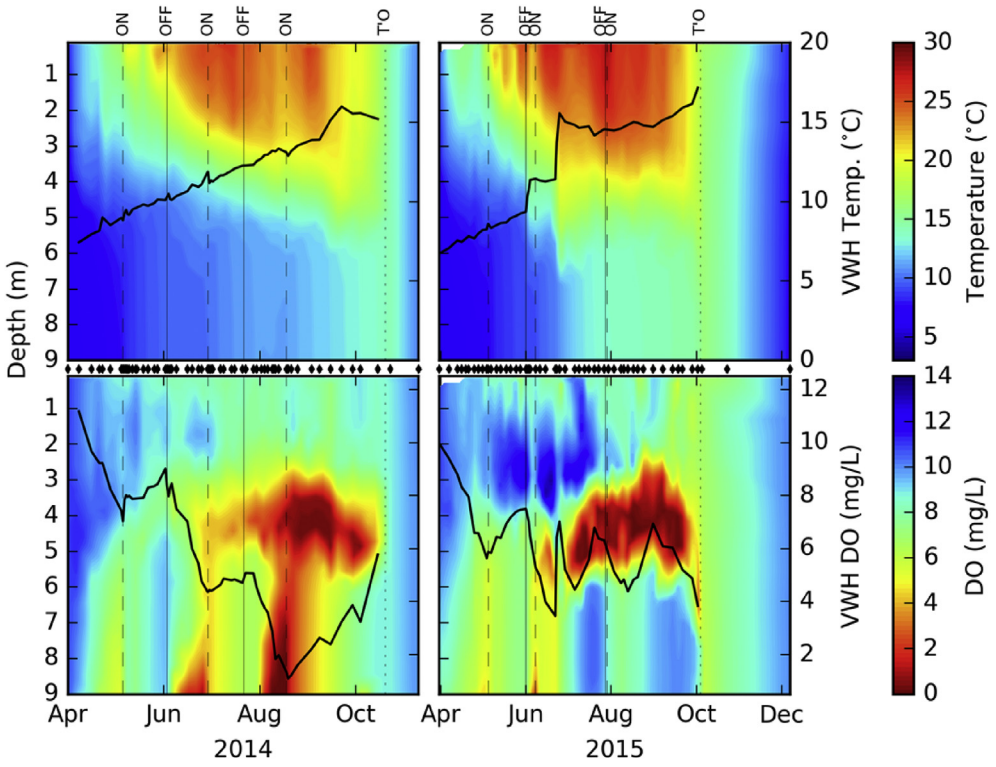

Fig. 3. Temperature (top) and DO concentrations (bottom) at the deepest location in FCR during 2014 (left) and 2015 (right). The volume-weighted hypolimnion temperature and volume-weighted hypolimnetic DO concentrations are shown as the solid line in the top and bottom panels, respectively. Sampling dates are shown as the black diamonds between panels, with linear interpolation between them. Vertical dashed lines indicate when the HOx was activated ('ON'), vertical solid lines indicate when the HOx system was deactivated ('OFF'), and the vertical dotted lines indicate the approximate date of reservoir destratification ('T/O').

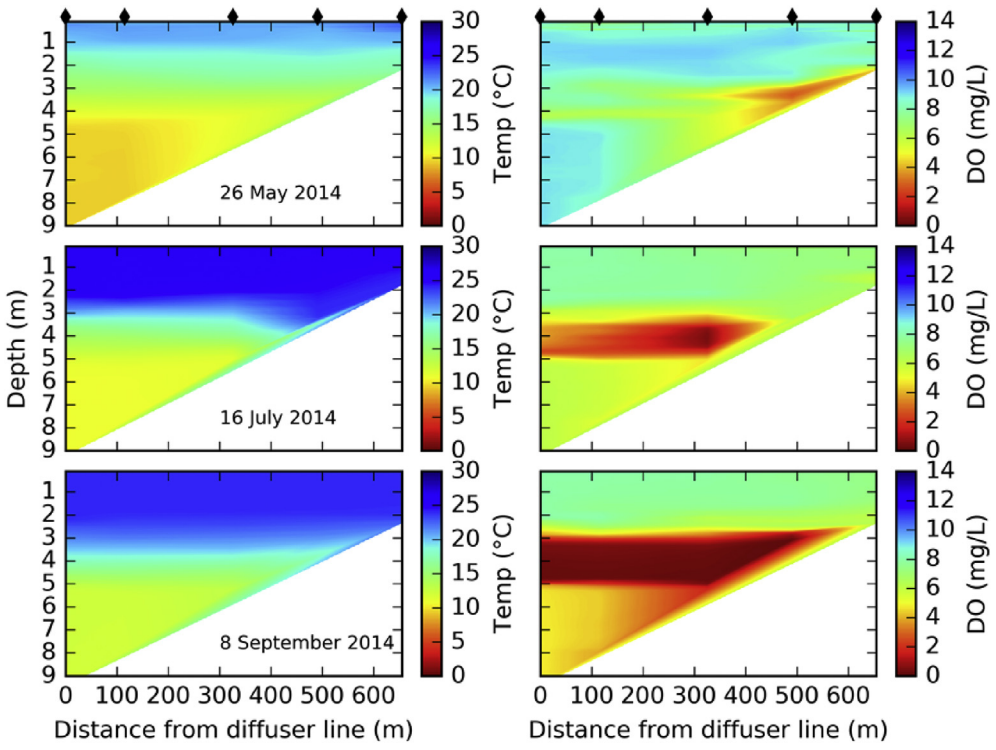

Fig. 4. Temperature (left) and DO concentrations (right) on a transect from the HOx system diffuser line to the northern portion of the reservoir (see Fig. 2): 26 May 2014 after the HOx system had been activated for 21 days (top), 16 July 2014 after the HOx system had been deactivated for 17 days (middle), and 8 September 2014 after the HOx system had been reactivated for 20 days (bottom).

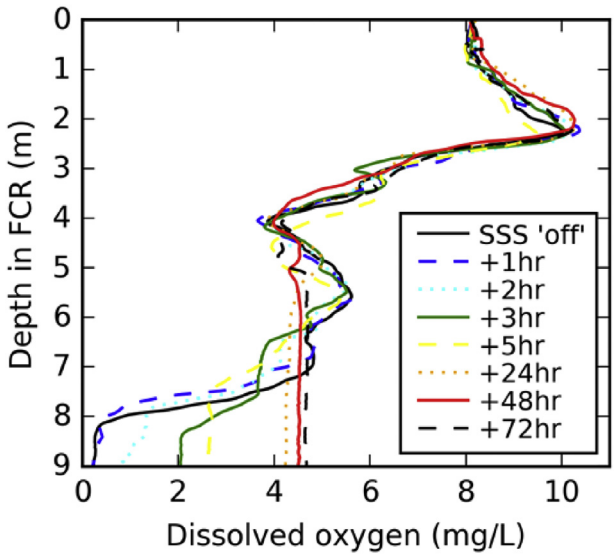

Fig. 5. Dissolved oxygen profiles at the deepest location in FCR immediately prior to activating the HOx on 29 June 2014 and at specified intervals afterwards: e.g., +1 h indicates the profile was collected 1 h after the HOx was activated.

throughout the hypolimnion when the HOx system was activated, even between June and September when we observed total Fe accumulating in the hypolimnion (Fig. 6). Soluble Fe was consistently <50% of the total Fe concentrations throughout the hypolimnion when the HOx system was activated, including measurements collected near the bottom of the reservoir; however, when anoxic conditions developed in response to HOx system deactivation in August 2014, soluble Fe increased to >90% of the total Fe concentrations measured in the bottom of the reservoir (9 m depth; Fig. 7). Within one week after the HOx system was reactivated in August 2014, soluble Fe at 9 m decreased to <50% of the total Fe concentration. Soluble Fe did not accumulate in the hypolimnion when the HOx system was activated; however, during the periods of HOx system deactivation in June and July–August 2014, the VWH soluble Fe concentrations increased by a mean rate of 0.007 ± 0.001 mg/L/d (Fig. 7), which was substantially lower than the accumulation rate measured for total Fe.

We observed increases in total and soluble Fe concentrations concurrent with the development of anoxia in the metalimnion in 2015 (Fig. 6). In July 2015, total Fe concentrations reached > 4 mg/L at 5 m depth (Fig. 7). By the end of August 2015, soluble Fe concentrations at 5 m decreased to ~1 mg/L and remained at or below this level until destratification, despite the persistence of anoxia in the metalimnion. However, total Fe remained elevated at 5 m between July–September (Fig. 7).

The rate of particulate Fe sedimentation increased as the VWH total Fe concentration increased over the summer stratified period in both 2014 and 2015 (Fig. 8). There was negligible change in particulate Fe sedimentation at 4 m during the summer stratified period, which averaged 0.16 ± 0.06 g/m^2/d during both years. The most significant changes in particulate sedimentation occurred in the 8 m trap. During the onset of thermal stratification, particulate Fe sedimentation at 8 m was < 0.2 g/m^2/d, but the flux reached > 2 g/m^2/d by August in both 2014 and 2015, despite differences in HOx system operation.

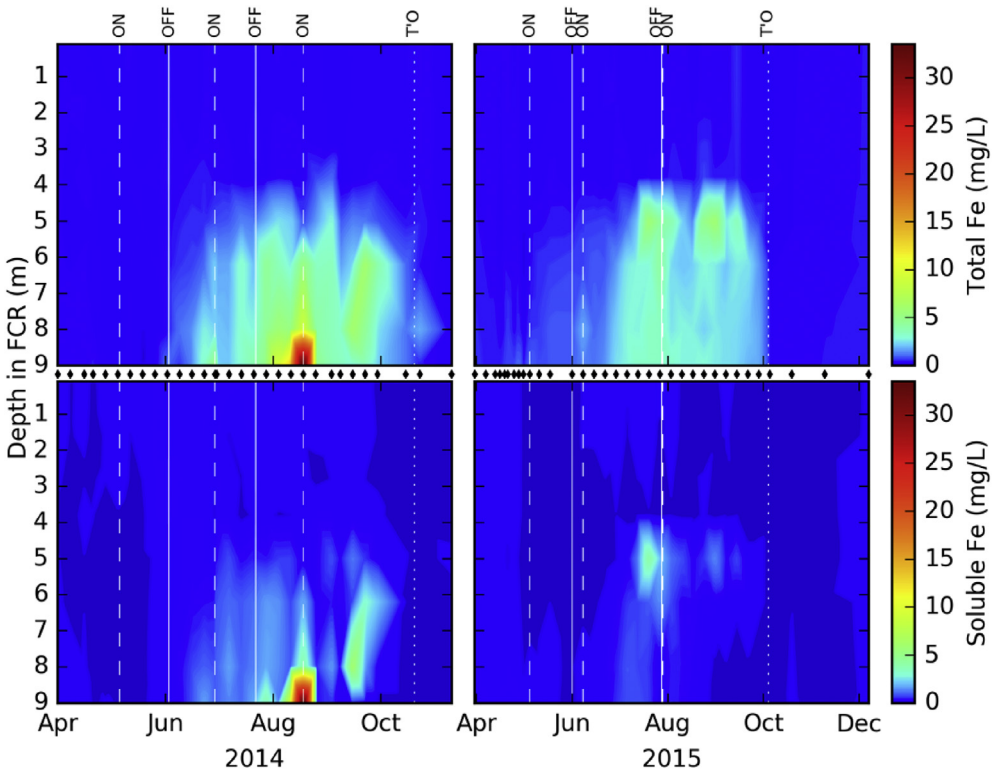

Fig. 6. Total (top) and soluble (bottom) Fe concentrations in FCR during 2014 (left) and 2015 (right). Samples were collected from nine depths in 2014 and seven depths in 2015; sampling dates are shown as the black diamonds between panels. The color map has been skewed to better illustrate patterns at concentrations <10 mg/L. Vertical dashed lines indicate when the HOx was activated ('ON'), vertical solid lines indicate when the HOx system was deactivated ('OFF') and the vertical dotted lines indicate the approximate date of reservoir destratification ('T/O').

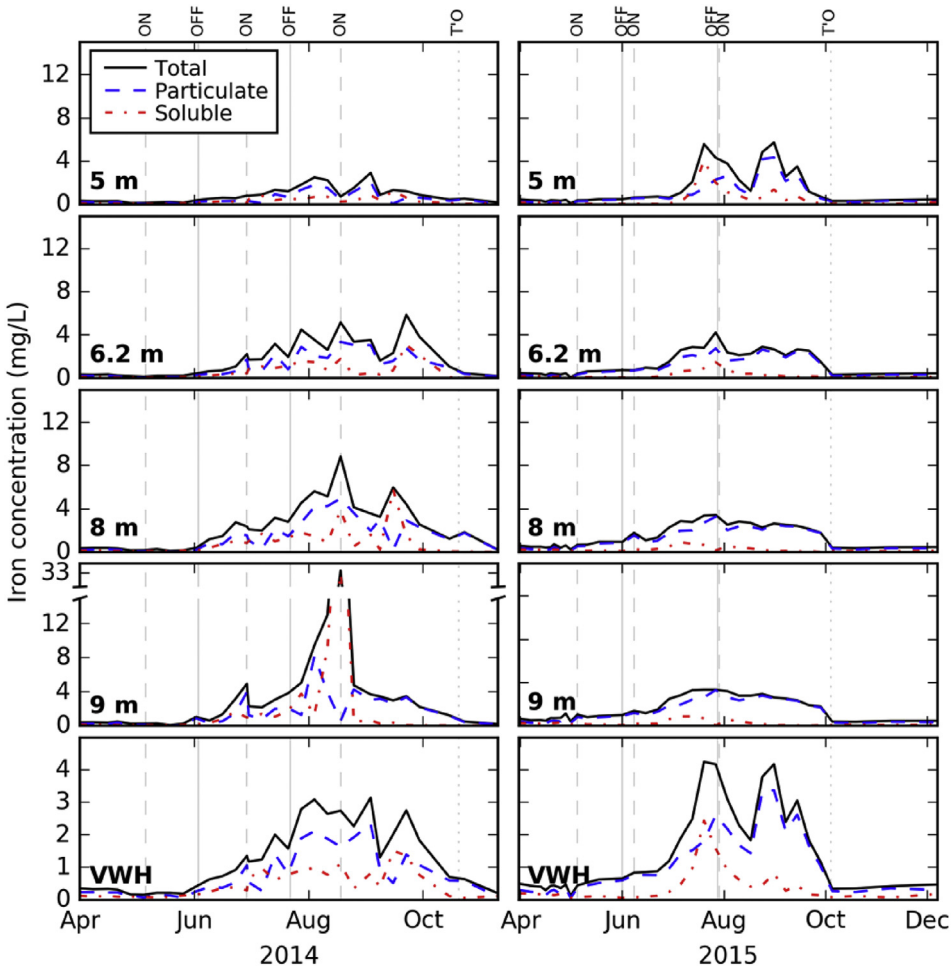

Fig. 7. Total (black solid line), particulate (blue dashed line) and soluble Fe (red dotted line) concentrations in the four hypolimnetic sample depths and the volume-weighted hypolimnetic Fe concentrations ('VWH') during 2014 (left) and 2015 (right). Vertical dashed lines indicate when the HOx was activated ('ON'), vertical solid lines indicate when the HOx system was deactivated ('OFF') and the vertical dotted lines indicate the approximate date of reservoir destratification ('T/O'). (For interpretation of the references to colour in this figure legend, the reader is referred to the web version of this article.)

3.3. Manganese concentrations in the reservoir water column and sedimentation traps

Similar to the Fe results, total Mn accumulated in the hypolimnion over the summer stratified period, regardless of HOx system operation (Fig. 9). During the early stratified period, between April and May, total Mn concentrations were <0.3 mg/L throughout the hypolimnion and did not substantially increase during these months in either year (Fig. 10). However, between June and September, the VWH total Mn concentration increased at rates of 0.009 mg/L/d and 0.010 mg/L/d in 2014 and 2015, respectively. Although total Mn accumulation in the hypolimnion occurred at similar rates in both years, we observed total Mn concentrations up to 4.1 mg/L during anoxia at 9 m depth in August 2014 (following a period of HOx system deactivation), which was much higher than total Mn concentrations measured anywhere in the hypolimnion during HOx system activation (Fig. 10).

In contrast to the Fe data, soluble Mn accumulated in the hypolimnion between June and September regardless of DO concentrations (Fig. 9). During these months in both years, the VWH soluble Mn constituted 89 ± 10% of the VWH total Mn concentration measurements on average (Fig. 10). When the HOx system was deactivated soluble Mn concentrations were much higher in the bottom of the reservoir (8 m and 9 m depths) than at shallower depths in the hypolimnion (Fig. 10). Immediately after HOx system reactivation the soluble Mn concentrations decreased rapidly at 8 m and 9 m. For example, reactivating the HOx system in both June and August 2014 caused the soluble Mn concentrations at 9 m depth to decrease by 47% and 39% within one week, respectively (Fig. 10). However, there was not a consistent pattern of decreasing soluble Mn concentrations throughout the hypolimnion; the VWH soluble Mn concentration decreased by 2% and increased by 53% one week after HOx system reactivation in June and August 2014, respectively. Furthermore, soluble Mn concentrations at 8 m and 9 m depths generally continued to increase in the weeks following HOx system activation, indicating that, similar to Fe, Mn also continued to be released from the sediments when the HOx system was activated (Fig. 10).

Particulate Mn sedimentation was higher in response to extended periods of HOx system activation in October 2014 and between July and September 2015 (Fig. 8). Mn sedimentation at 4 m exhibited a minor decrease between 2014 and 2015 (the mean sedimentation rates in 2014 and 2015 were 0.036 ± 0.014 g/m^2/d and 0.028 ± 0.014 g/m^2/d, respectively; Fig. 8). In 2014, Mn sedimentation at 8 m did not increase until late September, with the highest rate occurring after destratification. In 2015, particulate

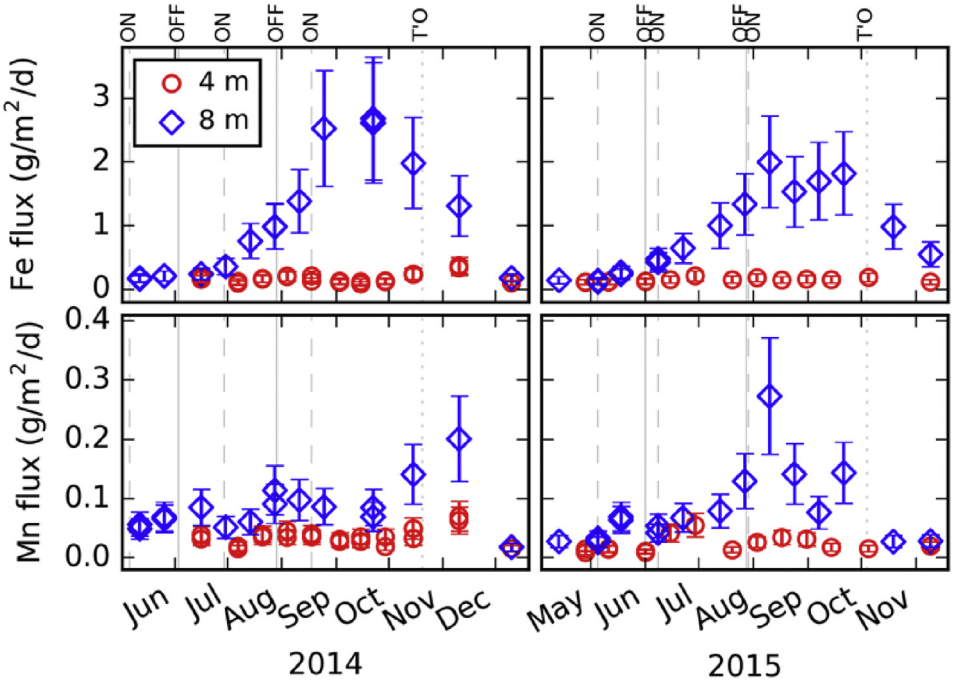

Fig. 8. Particulate Fe (top) and particulate Mn (bottom) flux at 4 m (red circles) and 8 m depth (blue diamonds) in FCR during 2014 (left) and 2015 (right). Samples were collected every 14–28 days and each data point represents the average daily flux over the preceding interval. Vertical dashed lines indicate when the HOx was activated ('ON'), vertical solid lines indicate when the HOx system was deactivated ('OFF'), and the vertical dotted lines indicate the approximate date of reservoir destratification ('T/O'). The error bars represent the standard deviation of replicate measurements. (For interpretation of the references to colour in this figure legend, the reader is referred to the web version of this article.)

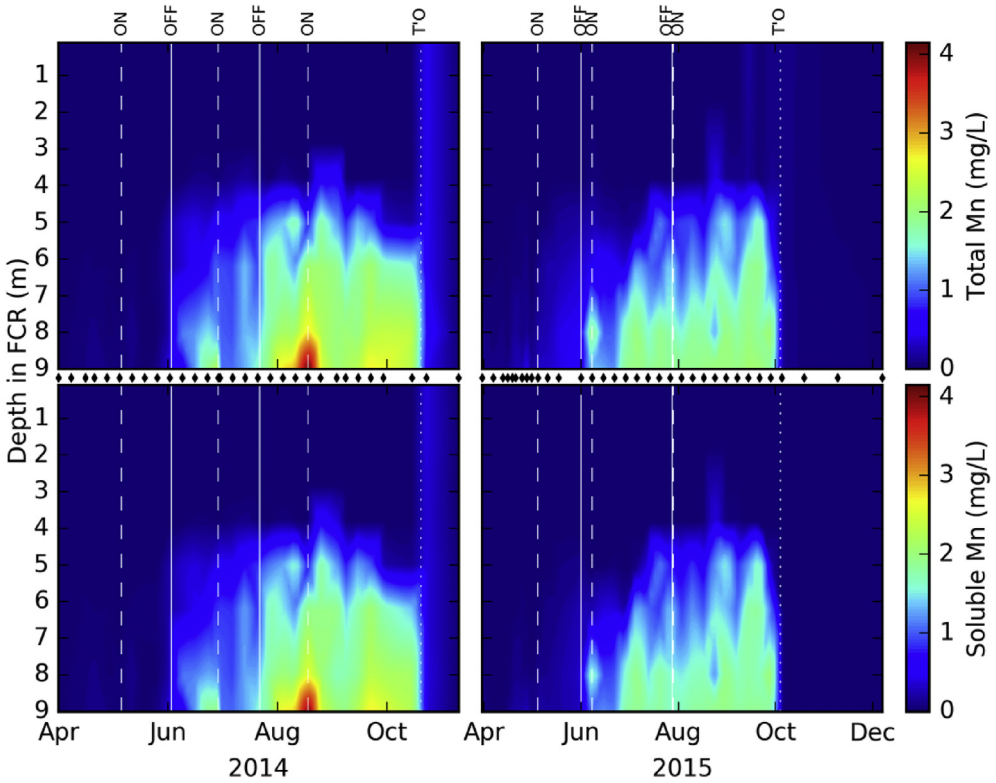

Fig. 9. Total (top) and soluble (bottom) Mn concentrations in FCR during 2014 (left) and 2015 (right). Samples were collected from nine depths in 2014 and seven depths in 2015; sampling dates are shown as the black diamonds between panels. Vertical dashed lines indicate when the HOx was activated ('ON'), vertical solid lines indicate when the HOx system was deactivated ('OFF') and the vertical dotted lines indicate the approximate date of reservoir destratification ('T/O').

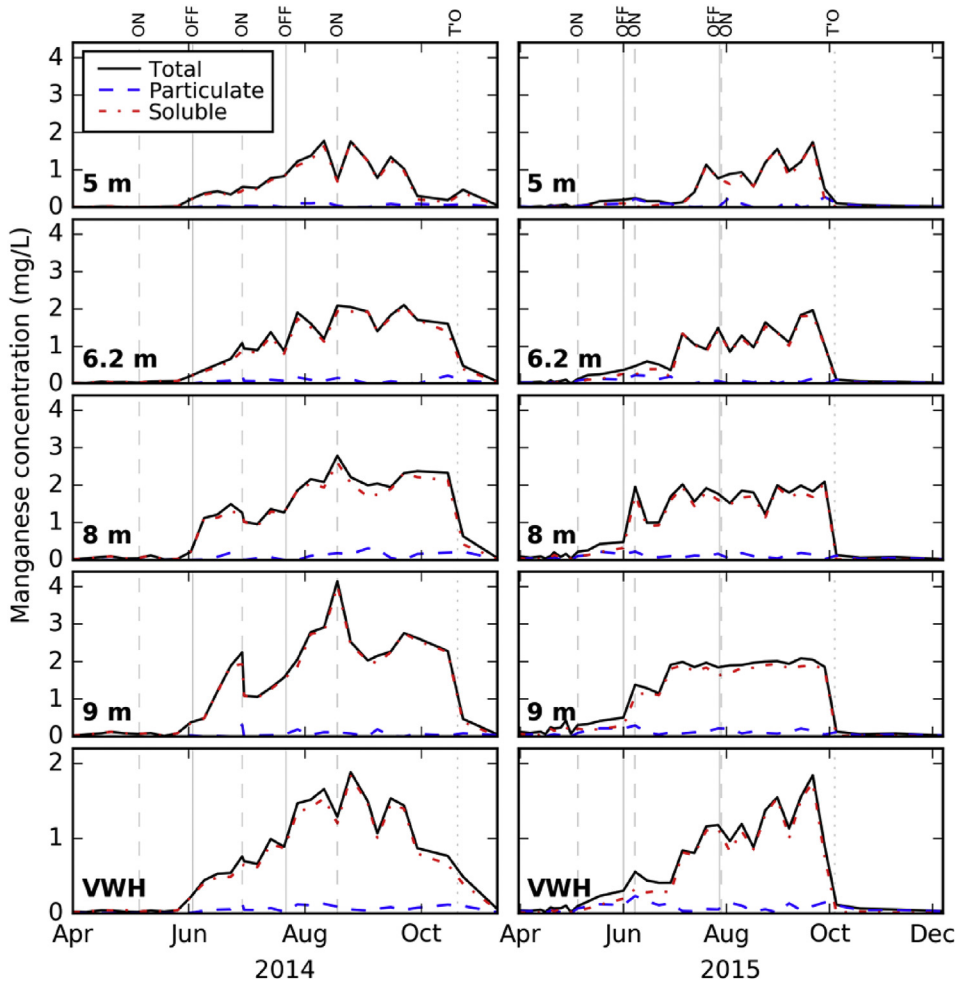

Fig. 10. Total (black solid line), particulate (blue dashed line) and soluble Mn (red dotted line) concentrations in the four hypolimnetic sample depths and the volume-weighted hypolimnetic Mn concentrations ('VWH') during 2014 (left) and 2015 (right). Vertical dashed lines indicate when the HOx was activated ('ON'), vertical solid lines indicate when the HOx system was deactivated ('OFF') and the vertical dotted lines indicate the approximate date of reservoir destratification ('T/O'). (For interpretation of the references to colour in this figure legend, the reader is referred to the web version of this article.)

Mn sedimentation increased earlier, in July, and remained elevated until reservoir destratification in October. Examination of the DO data revealed that the highest rates of particulate Mn sedimentation in the hypolimnion (8 m trap) occurred when DO concentrations were generally > 8 mg/L (Fig. 3).

We do not have data on the effects of oxygenation on sediment disturbance in the reservoir, but the design of the HOx system, which was constructed to minimize high flow rates at the sediments, historical records that show a rocky bottom in the hypolimnion (WVWA, unpublished data) and a lack of sediments observed within the Van Dorn sampler, suggest that sediment scouring during oxygenation was likely minimal.

3.4. Manganese incubation experiments

We observed soluble Mn oxidation only in the biologically active incubation experiments containing particulates and/or water from FCR (Fig. 11). The treatment containing live reservoir particulates (PMn) exhibited the greatest rate of soluble Mn removal at 0.042 mg/L/d, and the treatment containing live reservoir water (WMn) exhibited a lower removal rate of 0.0017 mg/L/d (Table 3). The sterilized treatments, consisting of particulates (SPMn) and reservoir water (SWMn), exhibited negligible change in soluble Mn concentration during the experiment. DO and pH conditions in the experiments (Table 2) were consistently maintained to reflect reservoir conditions. The mean DO concentration in the treatments was 8.3 ± 0.7 mg/L, similar to DO concentrations in well-oxygenated conditions of the hypolimnion in FCR; the mean pH in the flasks was 7.0 ± 0.7; within the pH range observed in the FCR water column (mean 6.6 ± 0.6).

3.5. Oxidation rates and half-times for soluble Fe and Mn in the hypolimnion

The half-time of soluble Fe in the water column of FCR was much shorter (~2 d) compared to soluble Mn (~15–33 d) in both years (Table 3 and Fig. 12). Our results showed that the mean half-time of soluble Fe in the hypolimnion of FCR was 1.6 ± 1.7 d over the summer stratified period in both 2014 and 2015, with negligible difference between years (Fig. 12). However, the half-time for soluble Mn was ~50% shorter over the summer stratified period in 2015 (15 ± 13 d), when the HOx system was continuously operated, compared to the same period in 2014 (33 ± 21 d), when the hypolimnion exhibited intermittent anoxia.

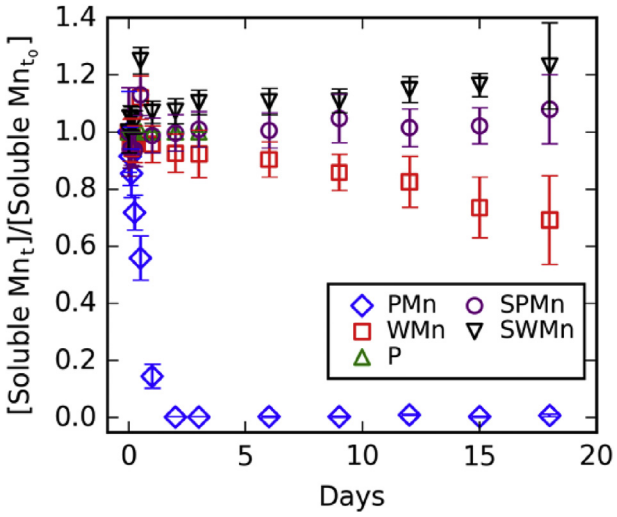

Fig. 11. Change in Mn concentration over time in incubation flasks containing reservoir particulates and water collected from the 4 m sedimentation traps deployed in FCR. The treatments included a slurry of reservoir particulates spiked with Mn (PMn), reservoir water spiked with Mn (WMn), a slurry of particulates without the Mn spike (P), a slurry of sterilized particulates spiked with Mn (SPMn), and sterilized reservoir water spiked with Mn (SWMn). Error bars represent the standard deviation of three replicate measurements. Experimental conditions are shown in Table 2.

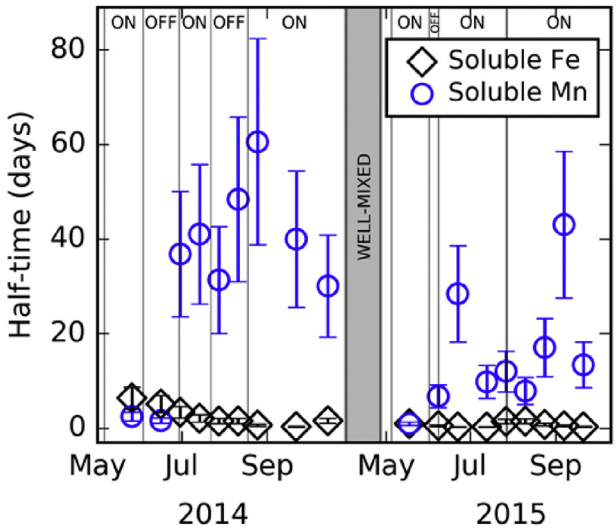

Fig. 12. Half-time of soluble Fe (black diamonds) and Mn (blue circles) in the hypolimnion of FCR during 2014 and 2015. The shaded area represents the well-mixed period between years. Vertical dashed lines indicate the transition between HOx system activation ('ON') and deactivation ('OFF'). (For interpretation of the references to colour in this figure legend, the reader is referred to the web version of this article.)

Table 2
Experimental conditions and calculated Mn oxidation half-times (t0.5) from the laboratory incubations. The treatments included a slurry of reservoir particulates spiked with Mn (PMn), reservoir water spiked with Mn (WMn), a slurry of particulates without the Mn spike (P), a slurry of sterilized particulates spiked with Mn (SPMn), and sterilized reservoir water spiked with Mn (SWMn). Half-times were not calculated for the P, SPMn, or SWMn treatments because there was a negligible decrease in the initial soluble Mn concentration. Values in parentheses are the standard deviation of the measurements over the 18 day-long experiment. Incubation flasks were kept at 22 °C.

Experiment	Mean DO (mg/L)	Mean pH	$t_{0.5}$ (days)
PMn	8.6(1.07)	6.7(0.35)	0.98
WMn	8.3(0.55)	6.6(0.32)	30
P	8.3(0.61)	6.8(0.22)	
SPMn	8.3(0.64)	8.2(0.22)	
SWMn	8.2(0.62)	6.9(0.40)	

4. Discussion

4.1. Effects of HOx system activation on Fe and Mn accumulation in the hypolimnion

Operation of the HOx system successfully prevented the accumulation of soluble Fe in the hypolimnion of FCR, but had little effect on soluble Mn accumulation. When the HOx system was activated, DO concentrations increased and became uniform throughout the hypolimnetic water column. Our results show that maintaining well-oxygenated conditions increased Fe oxidation, resulting in the formation of Fe-oxyhydroxides, to prevent significant soluble Fe accumulation in the water column (Fig. 6). However, under these same conditions, soluble Mn concentrations increased throughout the hypolimnion and persisted even in well-oxygenated zones (Fig. 9). Although the oxidation rate of soluble Mn increased when the HOx system was continuously activated in

Table 3
Summary of zero-order Mn oxidation rates in this study and collected from the published literature. All experiments were conducted under air-saturated conditions at room temperature. The initial Mn concentration, rate, and half-time values for the intermittent anoxia and well-oxygenated treatments are an average over the summer stratified period.

Reservoir	Mean pH	Initial Mn concentration (mg/L)	Mn oxidation rate (mg/L/d)	Half-time (d)	Experiment type	Sample treatment
FCR (this study)	6.7	1.69	0.86	0.98	Laboratory	Slurry of reservoir particulates
FCR (this study)	6.6	2.36	0.039	30	Laboratory	Reservoir water
FCR (this study)	6.8[d]	0.94	0.014	33	Field (reservoir-scale)	Intervals of HOx system deactivation in FCR (2014)
FCR (this study)	6.6	0.84	0.028	15	Field (reservoir-scale)	Continuous HOx system activation in FCR (2015)
Lake Zurich[a]	7.5	0.385	0.0058–0.084	2.3–33	Laboratory	Reservoir water spiked with "Mn-bacteria"
Lake Biwa[b]	7	0.100–0.750	0.0008–0.0021	1–3	Laboratory	Anoxic hypolimnetic waters aerated in the lab
Lake Oneida[c]	8–8.4	0.066	0.016	2.1	Laboratory	Hypolimnetic water

[a] Diem and Stumm (1984).
[b] Kawashima et al. (1988).
[c] Chapnick et al. (1982).
[d] pH measured at 6.2 m depth only.

2015 (Table 3), maintaining well-oxygenated conditions did not increase the rate of Mn oxidation enough to prevent soluble Mn accumulation in the hypolimnion.

The HOx system did not inhibit the accumulation of total Fe or Mn, which includes both the soluble and particulate fractions, during the summer stratified period in either year. The rate at which the VWH total Fe concentration increased over the summer stratified period exhibited little change when the HOx system was activated, suggesting that oxic conditions increased the rate of soluble Fe oxidation (conversion from soluble to particulate Fe), but did not suppress the release of Fe from the sediments and its accumulation in the overlying water column. Total Mn concentrations also increased over the summer stratified period reflecting the accumulation of soluble Mn, which constituted the majority of the total Mn concentrations (Fig. 9).

Our Mn results deviate from the findings of several other studies which support the effectiveness of hypolimnetic oxygenation for controlling Mn concentrations in selected source reservoirs (e.g., Bryant et al., 2011; Dent et al., 2014; Gantzer et al., 2009). We believe these contrasting results are due to the action of other processes besides Mn oxidation and differences in reservoir biogeochemistry that influence metal oxidation. For example, Dent et al. (2014) observed a 73% decrease in total Mn concentrations along a depth profile collected in North Twin Lake, 8 h after activating a bubble-plume HOx system; however, after one week, 94% of the Mn remained in soluble form, suggesting that mixing and dilution induced by the HOx system may have also influenced their observed Mn concentrations. Gantzer et al. (2009) reported a 97% decrease in the volume-weighted total Mn concentration in the bulk hypolimnion of Carvins Cove Reservoir after a year of continuous HOx system operation; however, the pH in Carvins Cove Reservoir is typically between 8 and 9 (Bryant et al., 2011), which is much more favorable for rapid Mn oxidation compared to the pH < 7 observed in FCR (Diem and Stumm, 1984; Hem, 1981; Morgan, 1967). The following discussion examines the role of DO, pH, and microorganisms in mediating the effects of HOx system operation on Fe and Mn concentrations.

4.1.1. Effects of DO, pH, and microorganisms on metal oxidation

The combined results of water column metal concentrations and sedimentation rates suggest that Fe oxidation was enhanced sufficiently during HOx system activation to prevent the accumulation of soluble Fe in the hypolimnion (Fig. 7), but that soluble Mn oxidation occurred more slowly, which allowed soluble Mn to accumulate in the hypolimnion even under well-oxygenated conditions (Fig. 10). Previous studies have demonstrated that oxidation of Fe and Mn is influenced by both DO concentration and pH; however, the oxidation rate of Fe is much faster than Mn at similar DO concentration and pH (Appelo and Postma, 2005; Millero et al., 1987; Morgan, 1967). For example, using the rate equation in Appelo and Postma (2005), the abiotic oxidation of soluble Fe at a DO concentration of 8.5 mg/L and pH 6.6, conditions observed in the hypolimnion of FCR, gives a half-time for soluble Fe of ~1.5 h. In contrast, using the rate equation for Mn in Morgan (1967) with the same pH and DO conditions, gives a half-time for soluble Mn of 10^5 days (approximately 275 years). The predicted half-time for soluble Fe under abiotic conditions is within the range of oxidation half-times calculated for Fe in the water column of FCR (half-time between 5 h and 7 d); however, the predicted half-time for soluble Mn under the same conditions was much longer than what we calculated in FCR (half-time < 60 d; Fig. 12; Table 3), indicating factors other than DO concentration and pH have a greater effect on Mn oxidation compared to Fe oxidation.

The concentration of hydrogen ions (pH) exerts a substantial effect on metal oxidation rates, but pH in the hypolimnion of FCR did not substantially change during the summer stratified period. For example, doubling DO concentration would cause the abiotic oxidation rate of Mn to double using the rate equation in Appelo and Postma (2005); however, doubling the hydrogen ion concentration would cause the abiotic oxidation rate to increase by a factor of four. Despite the comparatively larger effect of pH on abiotic metal oxidation, pH in the hypolimnion generally varied by less than 0.3 units and were slightly lower later in the summer stratified period, suggesting that the changes in metal oxidation rates calculated between the anoxic and well-oxygenated intervals between June and September were not substantially influenced by pH.

Our incubation experiment results show negligible abiotic Mn oxidation occurring at a DO concentration of ~8.5 mg/L and pH 6.6 within 18 d (Fig. 11). These results agreed with oxidation rates calculated using the rate equation in Morgan (1967); even at the highest DO concentration observed in FCR during the summer stratified period (10.5 mg/L), the predicted half-time for soluble Mn was > 10^4 d under abiotic conditions. At higher pH, between 8 and 9, the predicted half-time for soluble Mn would be between 1 and 100 d, suggesting that abiotic Mn oxidation may have been much faster if the pH in FCR were more alkaline, similar to the reservoirs studied in Bryant et al. (2011); Dent et al. (2014); and Gantzer et al. (2009).

Manganese oxidation occurred most rapidly in the biotic incubation treatments (Fig. 11). The oxidation half-time of soluble Mn in water collected from FCR (WMn treatment) was ~32 days, which is similar to results observed in previous studies conducted on oxic lake water samples (Table 3; Chapnick et al., 1982; Diem and Stumm, 1984; Kawashima et al., 1988; Tipping et al., 1984), and much shorter than the 10^5 days predicted from the abiotic oxidation rate equation. The half-time for soluble Mn measured in the particulates treatment was 50 times shorter than the reservoir water alone, suggesting that Mn-oxidizing organisms are concentrated in suspended particulates and that greater abundances can dramatically increase oxidation rates.

Higher DO concentrations in the hypolimnion in 2015 (Fig. 3) resulted in faster Mn oxidation compared to 2014 (Table 3 and Fig. 12). Although maintaining well oxygenated conditions would not substantially increase the abiotic rate of Mn oxidation, the faster oxidation rates observed in the hypolimnion suggest that higher DO concentrations may promote the oxidizing activity of Mn-oxidizing organisms (Fig. 12). It has been previously shown that DO is consumed proportionally to the production of oxidized Mn by *Leptothrix* bacteria (Boogerd and De Vrind, 1987); however, we do not know of any published literature that has demonstrated the effects of DO concentration on biotic Mn oxidation rates. Such a rate equation would be invaluable for optimizing future HOx system operation.

4.1.2. Implications for controlling Fe and Mn with hypolimnetic oxygenation

Our results show that continuous operation of the HOx system during the summer stratified period is essential to optimizing its effectiveness for controlling soluble metals. Continual operation of the HOx system prevented the development of anoxic zones in the hypolimnion where we observed the highest concentrations of soluble Fe in 2014 (Fig. 7); when the HOx system was continuously operated, soluble Fe did not accumulate near the benthic sediments where we had previously measured soluble Fe concentrations >30 mg/L. Although soluble Mn still accumulated under well-oxygenated conditions, the concentrations near the benthic sediments were twice as high when anoxia was allowed to develop (Fig. 10). Hypolimnetic oxygenation effectively prevented soluble Fe accumulation, even under slightly acidic conditions, because of the

fast oxidation kinetics of Fe. The oxidation of Mn is generally slower and is sensitive to pH and microbial activity, but the shorter oxidation half-times calculated for soluble Mn during continual operation of the HOx system suggests that maintaining high DO concentrations (>8 mg/L) is also useful for stimulating the oxidation and removal of soluble Mn. Accumulation of soluble Mn in the water column in FCR in both 2014 and 2015 reflects the relatively slow oxidation kinetics that are inherent to Mn.

Results of the incubation experiment support previous work showing that biotic activity, likely resulting from the presence of Mn-oxidizing microorganisms, is a key part of the Mn redox cycle in natural systems and thus are critical elements of engineered systems to treat Mn *in situ*. Additional work is needed to identify the community of metal-oxidizing organisms, their distribution in the water column, and the optimal DO concentration and pH needed to maximize their oxidizing behavior in FCR.

5. Conclusions

The goal of this study was to investigate the effects of hypolimnetic oxygenation on Fe and Mn dynamics in a shallow, dimictic drinking water reservoir. Overall, our results showed that hypolimnetic oxygenation was effective for controlling soluble Fe. However, although continuous operation of the HOx system increased the rate of Mn oxidation, soluble Mn accumulated in the water column. Several other patterns emerged from our results in FCR that are important for water quality management: 1) Increasing DO concentrations to > 8 mg/L maximized the rate of soluble Mn oxidation in the hypolimnion. 2) The rate of Mn oxidation in the water column is likely influenced by the presence of Mn-oxidizing organisms that are associated with water column particulates. 3) Although the HOx system maintained oxidizing conditions in the hypolimnion, it did not prevent the continued release of Fe and Mn from the sediments, thus limiting its effectiveness to the rate at which metals may oxidize in the water column. In summary, hypolimnetic oxygenation may be a favorable management strategy for controlling soluble Fe, but future work is needed to optimize it effectiveness in promoting soluble Mn oxidation.

Acknowledgements

We thank the reviewers and the editor for their insightful comments that greatly improved the manuscript. We thank the staff at the Western Virginia Water Authority for their long-term support and funding. In particular, we would like to thank Cheryl Brewer, Jamie Morris, Jeff Booth, Bob Benninger, and Gary Robertson. Jeffrey Parks, Mariah Redmond, Mariah Haberman, Madeline Ryan, Charlotte Harrell, Athena Tilley, and Bobbie Niederlehner provided critical help in the field and laboratory. We also thank Don Rimstidt for help in modeling metal oxidation rates. This work was supported by the Institute for Critical Technology and Applied Science at Virginia Tech, Virginia Tech Global Change Center, and Fralin Life Sciences Institute.

Appendix A. Supplementary data

Supplementary data related to this article can be found at http://dx.doi.org/10.1016/j.watres.2016.09.038.

References

Aguilar, C., Nealson, K.H., 1998. Biogeochemical cycling of manganese in Oneida Lake, New York: whole lake studies of manganese. J. Gt. Lakes Res. 24, 93–104.
American Public Health Association, American Water Works Association, Water Environment Federation, 1998. Standard Methods for the Examination of Water and Wastewater, twentieth ed. American Public Health Association, Washington, DC.
Appelo, C.A.J., Postma, D., 2005. Geochemistry, Groundwater and Pollution, second ed. CRC press, Boca Raton, Florida.
Beutel, M.W., Horne, A.J., 1999. A review of the effects of hypolimnetic oxygenation on lake and reservoir water quality. Lake Reserv. Manag. 15, 285–297.
Beutel, M.W., Leonard, T.M., Dent, S.R., Moore, B.C., 2008. Effects of aerobic and anaerobic conditions on P, N, Fe, Mn, and Hg accumulation in waters overlaying profundal sediments of an oligo-mesotrophic lake. Water Res. 42, 1953–1962.
Boogerd, F., De Vrind, J., 1987. Manganese oxidation by Leptothrix discophora. J. Bacteriol. 169, 489–494.
Bryant, L.D., Hsu-Kim, H., Gantzer, P.A., Little, J.C., 2011. Solving the problem at the source: controlling Mn release at the sediment-water interface via hypolimnetic oxygenation. Water Res. 45, 6381–6392.
Burdige, D.J., 1993. The biogeochemistry of manganese and iron reduction in marine sediments. Earth-Sci. Rev. 35, 249–284.
Burns, F.L., 1998. Case study: automatic reservoir aeration to control manganese in raw water Maryborough town water supply Queensland, Australia. Water Sci. Technol. 37, 301–308.
Chapnick, S.D., Moore, W.S., Nealson, K.H., 1982. Microbially mediated manganese oxidation in a freshwater lake1. Limnol. Oceanogr. 27, 1004–1014.
Creed, J., Brockhoff, C., Martin, T., 1994. Method 200.8: Determination of Trace Elements in Waters and Wastes by Inductively-coupled Plasma-mass Spectrometry, fifth ed. Environmental Monitoring Systems Laboratory, Office of Research and Development, US Environmental Protection Agency, Cincinnati, Ohio.
Davison, W., 1993. Iron and manganese in lakes. Earth-Sci. Rev. 34, 119–163.
Debroux, J.-F., Beutel, M.W., Thompson, C.M., Mulligan, S., 2012. Design and testing of a novel hypolimnetic oxygenation system to improve water quality in Lake Bard, California. Lake Reserv. Manag. 28, 245–254.
Dent, S.R., Beutel, M.W., Gantzer, P., Moore, B.C., 2014. Response of methylmercury, total mercury, iron and manganese to oxygenation of an anoxic hypolimnion in North Twin Lake, Washington. Lake Reserv. Manag. 30, 119–130.
Diem, D., Stumm, W., 1984. Is dissolved Mn 2+ being oxidized by O2 in absence of Mn-bacteria or surface catalysts? Geochim. Cosmochim. Acta 48, 1571–1573.
Gantzer, P.A., Bryant, L.D., Little, J.C., 2009. Controlling soluble iron and manganese in a water-supply reservoir using hypolimnetic oxygenation. Water Res. 43, 1285–1294.
Gerling, A.B., Browne, R.G., Gantzer, P.A., Mobley, M.H., Little, J.C., Carey, C.C., 2014. First report of the successful operation of a side stream supersaturation hypolimnetic oxygenation system in a eutrophic, shallow reservoir. Water Res. 67, 129–143.
Gerling, A.B., Munger, Z.W., Doubek, J.P., Hamre, K.D., Gantzer, P.A., Little, J.C., Carey, C.C., 2016. Whole-catchment manipulations of internal and external loading reveal the sensitivity of a century-old reservoir to hypoxia. Ecosystems 19, 555–571.
Hem, J.D., 1981. Rates of manganese oxidation in aqueous systems. Geochim. Cosmochim. Acta 45, 1369–1374.
Hem, J.D., 1972. Chemical factors that influence the availability of iron and manganese in aqueous systems. Geol. Soc. Am. Spec. Pap. 140, 17–24.
Hongve, D., 1997. Cycling of iron, manganese, and phosphate in a meromictic lake. Limnol. Oceanogr. 42, 635–647.
Jones, B.F., Bowser, C.J., 1978. The mineralogy and related chemistry of lake sediments. In: Lakes. Springer, New York, pp. 179–235.
Kawashima, M., Takamatsu, T., Koyama, M., 1988. Mechanisms of precipitation of manganese (II) in Lake Biwa, a fresh water lake. Water Res. 22, 613–618.
Kohl, P.M., Medlar, S.J., 2006. Occurrence of Manganese in Drinking Water and Manganese Control. American Water Works Association, Denver, Colorado.
Lerman, A., Imboden, D., Gat, J., 1995. Physics and Chemistry of Lakes, second ed. Springer, New York.
Lovley, D.R., 1987. Organic matter mineralization with the reduction of ferric iron: a review. Geomicrobiol. J. 5, 375–399.
Millero, F.J., Sotolongo, S., Izaguirre, M., 1987. The oxidation kinetics of Fe (II) in seawater. Geochim. Cosmochim. Acta 51, 793–801.
Morgan, J.J., 1967. Chemical equilibria and kinetic properties of manganese in natural waters. In: Principles and Applications of Water Chemistry. Wiley, New York, pp. 561–624.
Nealson, K.H., Saffarini, D., 1994. Iron and manganese in anaerobic respiration: environmental significance, physiology, and regulation. Annu. Rev. Microbiol. 48, 311–343.
Read, J.S., Hamilton, D.P., Jones, I.D., Muraoka, K., Winslow, L.A., Kroiss, R., Wu, C.H., Gaiser, E., 2011. Derivation of lake mixing and stratification indices from high-resolution lake buoy data. Environ. Model. Softw. 26, 1325–1336.
Richardson, L.L., Aguilar, C., Nealson, K.H., 1988. Manganese oxidation in pH and O2 microenvironments produced by phytoplankton1, 2. Limnol. Oceanogr. 33, 352–363.
Rimstidt, J.D., 2013. Geochemical Rate Models: an introduction to geochemical kinetics, first ed. Cambridge University Press, New York.
Singleton, V.L., Little, J.C., 2006. Designing hypolimnetic aeration and oxygenation systems-a review. Environ. Sci. Technol. 40, 7512–7520.
Sommerfeld, E.O., 1999. Iron and Manganese Removal Handbook, first ed. American Water Works Association, Denver, Colorado.
Tebo, B.M., Johnson, H.A., McCarthy, J.K., Templeton, A.S., 2005. Geomicrobiology of manganese (II) oxidation. TRENDS Microbiol. 13, 421–428.
Tipping, E., Thompson, D., Davison, W., 1984. Oxidation products of Mn (II) in lake

waters. Chem. Geol. 44, 359–383.
United States Environmental Protection Agency, 2016. Table of Regulated Drinking Water Contaminants [WWW Document]. https://www.epa.gov/ground-water-and-drinking-water/table-regulated-drinking-water-contaminants (accessed 6.6.16).
United States Environmental Protection Agency, 1995. Method 3051: microwave assisted acid digestion of sediments, sludges, soils, and oils. In: Test Methods for Evaluating Solid Waste. United States Environmental Protection Agency, Washington, D.C.
Wasserman, G.A., Liu, X., Parvez, F., Ahsan, H., Levy, D., Factor-Litvak, P., Kline, J., van Geen, A., Slavkovich, V., Lolacono, N.J., et al., 2006. Water manganese exposure and children's intellectual function in Araihazar, Bangladesh. Environ. Health Perspect. 124–129.
World Health Organization, 2004. Guidelines for Drinking-water Quality: Recommendations, third ed. World Health Organization, Geneva, Switzerland.
Zaw, M., Chiswell, B., 1999. Iron and manganese dynamics in lake water. Water Res. 33, 1900–1910.